Dynamic polarizabilities and magic wavelengths for dysprosium

V. A. Dzuba and V. V. Flambaum
School of Physics, University of New South Wales, Sydney, New South Wales 2052, Australia

Benjamin L. Lev
Department of Physics, University of Illinois at Urbana-Champaign, Urbana, Illinois 61801-3080, USA

(Received 22 November 2010; published 4 March 2011)

We theoretically study dynamic scalar polarizabilities of the ground and select long-lived excited states of dysprosium, a highly magnetic atom recently laser cooled and trapped. We demonstrate that there is a set of magic wavelengths of the unpolarized lattice laser field for each pair of states, which includes the ground state and one of these excited states. At these wavelengths, the energy shift due to laser field is the same for both states, which can be useful for resolved sideband cooling on narrow transitions and precision spectroscopy. We present an analytical formula that, near resonances, allows for the determination of approximate values of the magic wavelengths without calculating the dynamic polarizabilities of the excited states.

DOI: 10.1103/PhysRevA.83.032502 PACS number(s): 31.15.am, 32.70.Cs, 31.30.jg, 37.10.De

I. INTRODUCTION

The dysprosium atom has many unique features, which makes it useful for studying fundamental problems of modern physics. This is a heavy atom that has many stable Bose and Fermi isotopes (from $A = 156$ to $A = 164$) and a pair of almost-degenerate states of opposite parity at $E = 19\,798$ cm^{-1}. These features were used to study the parity nonconservation [1–5] and possible time variation of the fine-structure constant [6–12].

Fermionic Dy has the largest magnetic moment among all atoms, and only Tb is as magnetic as bosonic Dy. This opens important opportunities for studying strongly correlated matter when gases of Dy atoms are cooled to ultracold temperatures [13]. Recent progress in Doppler and sub-Doppler cooling is an important step in this direction [13–17]. In addition to narrow-line magneto-optical trapping (MOT) [18], further cooling on narrow optical transitions might be possible using resolved-sideband cooling [19,20].

In this method, vibrational states of the atom may be coupled such that successive photon absorption and spontaneous emission cycles reduce the vibrational quanta by one, until the atoms are in the motional ground state of their optical potential [19]. It is important that this resolved-sideband cooling is performed at the *magic* wavelength of the laser lattice field [21,22]. At this wavelength, the energy (ac Stark) shift due to the laser field is the same for both states used in the cooling. This results in a trap potential that is the same for both states, and optical transitions between vibrational states can be well resolved. This allows spectral selection of cooling transitions, those which remove one vibrational quanta, without contamination by heating transitions, which add vibrational quanta. Other benefits to optical trapping at magic wavelengths include enhanced precision spectroscopy and longer-lived quantum memory for quantum information processing (QIP) [21].

In this paper we calculate dynamic polarizabilities of the ground and three long-lived excited states of Dy and present a number of magic wavelengths for the transitions between them. We also present an analytical formula that allows the determination of approximate values of the magic wavelengths near resonances without calculating the dynamic polarizabilities of excited states. The optical field is assumed to be unpolarized, although we estimate that polarization would induce only small shifts in the magic wavelengths.

II. CALCULATIONS

A. *Ab initio* calculations

The dynamic scalar polarizability α_a of atomic state a is given by (we use atomic units: $\hbar = 1, m_e = 1, |e| = 1$)

$$\alpha_a(\omega) = -\frac{1}{3(2J_a+1)}\sum_n \times \left[\frac{1}{E_a - E_n + \omega} + \frac{1}{E_a - E_n - \omega}\right] \langle a||\mathbf{D}||n\rangle^2, \tag{1}$$

where J_a is total momentum of state a, E_a is its energy, and $\mathbf{D} = -\sum_i \mathbf{r_i}$ is the electric dipole operator. Summation goes over the complete set of excited states n.

We use the relativistic configuration interaction (CI) technique described in our previous papers [5,11,23] to perform the calculations. The single-electron and many-electron basis sets, the fitting parameters, and other details of present calculations are exactly the same as in Ref. [5]. This simple method provides a good accuracy for low-lying states of a many-electron atom. However, it does not allow for the saturation of the summation in Eq. (1) over a complete set of many-electron states. On the other hand, the contribution of the higher-lying states in the dynamic polarizability does not depend on frequency at small frequencies. Therefore, for small frequencies we can rewrite Eq. (1) as

$$\alpha_a(\omega) = \tilde{\alpha}_a - \frac{1}{3(2J_a+1)}\sum_{n'} \times \left[\frac{1}{E_a - E_{n'} + \omega} + \frac{1}{E_a - E_{n'} - \omega}\right] \langle a||\mathbf{D}||n'\rangle^2, \tag{2}$$

where the summation is over a limited number of low-lying near-resonant states and a constant $\tilde{\alpha}_a$ is chosen in such a way that Eq. (2) at $\omega = 0$ provides the correct value of the polarizability.

Dysprosium ground-state static polarizability is known to be 166 a_B^3 [24]. Static polarizabilities of excited states are not known and need to be calculated. We use an approximate approach in which the dysprosium atom is treated as a closed-shell system and the effect of electron vacancies in the open shells is taken into account via fractional occupation numbers. The static polarizability of a closed-shell system is given by

$$\alpha_a(0) = -\frac{2}{3}\sum_{cn}\frac{\langle c||\mathbf{D}||n\rangle^2}{\epsilon_c - \epsilon_n}, \tag{3}$$

where the summation is over a complete set of single-electron states, including states in the core (c) and states above the core (n). Electric dipole matrix elements are calculated using relativistic Hartree-Fock and Hartree-Fock in external field approximations [25]. Note that core polarization needs to be included only in one of two electric dipole matrix elements in (3) (see, e.g., Ref. [26] for details).

We use the standard B-spline technique [27] to generate a complete set of single-electron states. An additional term is included in the Hartree-Fock Hamiltonian to simulate the effect of correlations. This term has the form

$$\delta V(r) = -\frac{d}{2\left(r_0^4 + r^4\right)}, \tag{4}$$

where r_0 is a cutoff parameter (we use $r_0 = 1\ a_B$) and d is dipole polarizability of the core. We treat d as a fitting parameter and choose it to fit the known polarizability of dysprosium's ground state ($166a_0^3$ [24]), which results in $d = 3.7\ a_B^3$.

Then we perform similar calculations for the excited states of the $4f^9 6s^2 5d$ configuration, resulting in a calculated value of the static polarizability of 114 a_B^3. Note that this approach does not distinguish between different states of the same configuration. Therefore, static polarizabilities of all these states are assumed to be equal. This is only true for the static polarizabilities. Dynamic polarizabilities are different for different states due to contributions of the near-resonant states in Eq. (2).

In the present paper we consider dynamic polarizabilities of four states of dysprosium: the even ground state (GS) and three odd long-lived excited states. The first excited state is $^7\mathrm{H}_8^o$ at $\lambda = 1322$ nm ($E = 7565.60\ \mathrm{cm}^{-1}$), and we denote it as O1 for reference. This state is in the telecommunications band and could be used for hybrid atom-photon telecom quantum information networks. The second excited state is the $^7\mathrm{I}_9^o$ state at 1001 nm (9990.95 cm^{-1}), which we denote as O2. Quantum dots (QDs) emit in this wavelength range, allowing for the possibility of hybrid quantum circuits of QD single-photon emitters coupled to neutral atom-based long-lived quantum memory. O3 is the $^5\mathrm{K}_9^o$ state at 741 nm (13 495.92 cm^{-1}), which is a closed cycling transition with a linewidth [28] optimal for creating a narrow-line MOT. States O2 and O3 could also be useful for resolved-sideband cooling, as discussed below.

TABLE I. Electric dipole transition amplitudes (reduced matrix elements in atomic units) used for calculating the dynamic polarizability of the Dy ground state $^5\mathrm{I}_8$.

State n			
Configuration	Term	E_n (cm^{-1})	$\lvert A_{na}\rvert$(a.u.)[a]
$4f^9 5d6s^2$	$^7\mathrm{H}_8^o$	7565	0.061
$4f^9 5d6s^2$	$^7\mathrm{H}_7^o$	8519	0.124
$4f^9 5d6s^2$	$^7\mathrm{I}_9^o$	9990	0.059
$4f^9 5d6s^2$	$^7\mathrm{I}_8^o$	12 007	0.573
$4f^9 5d6s^2$	$^7\mathrm{G}_7^o$	12 655	0.108
$4f^9 5d6s^2$	$^5\mathrm{K}_9^o$	13 495	0.424
$4f^9 5d6s^2$	$^7\mathrm{I}_7^o$	14 367	0.475
$4f^9 5d6s^2$	$^5\mathrm{I}_8^o$	14 625	1.828
$4f^9 5d6s^2$	$^5\mathrm{H}_7^o$	15 194	1.452
$4f^{10} 6s6p$	$(8,0)_8^o$	15 567	0.464
$4f^{10} 6s6p$	$(8,1)_9^o$	15 972	1.365
$4f^9 5d6s^2$	$^7\mathrm{K}_8^o$	16 288	0.182
$4f^{10} 6s6p$	$(8,1)_7^o$	16 693	1.842
$4f^{10} 6s6p$	$(8,1)_8^o$	16 733	0.633
$4f^9 5d6s^2$	$^7\mathrm{K}_9^o$	16 717	0.415
$4f^9 5d6s^2$	$^7\mathrm{K}_7^o$	17 687	0.763
$4f^{10} 6s6p$	$(8,2)_9^o$	17 727	0.897
$4f^{10} 6s6p$	$(8,2)_8^o$	18 021	0.684
$4f^{10} 6s6p$	$(8,2)_7^o$	18 433	0.636
$4f^9 5d^2 6s$	$^9\mathrm{G}_7^o$	18 528	0.067
$4f^9 5d^2 6s$	$^7\mathrm{H}_9^o$	19 557	0.036
$4f^9 5d6s^2$	$^5\mathrm{K}_8^o$	19 688	0.627
$4f^9 5d^2 6s$	$^7\mathrm{G}_9^o$	21 540	0.523
$4f^{10} 6s6p$	$(7,2)_9^o$	21 838	0.513
$4f^9 5d^2 6s$	$?_9^o$	23 271	0.003
$4f^{10} 6s6p$	$(8,1)_9^o$	23 737	12.277

[a] $A_{na} \equiv \langle n||\mathbf{D}||a\rangle$.

We calculate dynamic polarizabilities using Eq. (1) in which we substitute transition amplitudes found from the CI calculations [5] and experimental energies. We use theoretical values in the few cases where experimental energies are not available. Tables I and II show calculated electric dipole transition amplitudes (reduced matrix elements) used in the calculations. The data from Table II can be used to calculate the lifetimes of the three excited states. The results are 5.2 ms for O1, 2.7 ms for O2, and 21 μs for O3, although O3 has recently been measured to be 89.3 μs [28].

Figures 1, 2, and 3 show dynamic polarizabilities of three pairs of states: GS and O1 (Fig. 1), GS and O2 (Fig. 2), and GS and O3 (Fig. 3). Lines crossing indicates that energy shifts of two states in a laser field are identical, and atoms have the same oscillation frequency in optical dipole traps at this wavelength regardless of whether they are in their ground or excited state. These so-called *magic* wavelengths occur most often very close to narrow resonances.

B. Simple estimations

In this subsection we present a way of estimating magic wavelengths for complex atoms in the vicinity of narrow resonances. Although all magic wavelengths presented in this work are found by the many-body calculations, the formulas in this subsection can be used to find more magic wavelengths

TABLE II. Electric dipole transition amplitudes (reduced matrix elements in atomic units) used for calculating the dynamic polarizabilities of the selected three long-lived Dy excited states.

State n			$\lvert A_{na}\rvert$[a] (a.u.)		
Configuration	Term	E_n(cm^{-1})	O1[b]	O2[c]	O3[d]
$4f^{10}6s^2$	$^5\mathrm{I}_8$	0	0.061	0.059	0.424
$4f^{10}6s^2$	$^5\mathrm{I}_7$	4134	0.007		
$4f^{10}5d6s$	$^3[8]_9$	17 515	0.033	0.154	0.139
$4f^{10}5d6s$	$^3[7]_8$	17 613	0.195	0.321	0.046
$4f^{10}5d6s$	$^3[6]_7$	18 095	0.170		
$4f^{10}5d6s$	$^3[9]_{10}$	18 463		0.060	0.210
$4f^{10}5d6s$	$^3[8]_8$	18 903	0.300	0.401	0.268
$4f^{10}5d6s$	$^3[7]_7$	18 938	0.259		
$4f^{10}6s^2$	$^3\mathrm{K}2_8$	19 019	0.083	0.093	0.064
$4f^{10}5d6s$	$^3[9]_9$	19 241	0.079	0.119	0.015
$4f^{10}5d6s$	$^3[10]_{10}$	19 798		0.049	0.192
$4f^{10}5d6s$	$^3[9]_8$	20 194	0.358	0.336	0.288
$4f^{10}5d6s$	$^3[10]_9$	20 209	0.041	0.062	0.010
$4f^9 6s^2 6p$	$(\frac{15}{2},\frac{1}{2})_7$	20 614	2.164		
$4f^9 6s^2 6p$	$(\frac{15}{2},\frac{1}{2})_8$	20 790	3.737	4.254	2.911
$4f^{10}5d6s$	$^3[8]_7$	21 074	0.550		
$4f^{10}5d6s$	$^3[7]_8$	21 603	0.362	0.450	0.130
$4f^{10}5d6s$	$^3[6]_7$	21 778	0.463		
$4f^{10}5d6s$	$^1[9]_9$	22 046	0.079	0.081	0.116
$4f^{10}5d6s$	$^1[9]_{10}$	22 487		0.004	0.112
$4f^9 5d6s6p$	$?_9$	23 219	1.313	3.879	0.400
$4f^{10}5d6s$	$?_7$	23 361	0.172		

[a] $A_{na} \equiv \langle n||\mathbf{D}||a\rangle$.
[b] State $a = 4f^9 5d6s^2, {}^7\mathrm{H}^o_8$, $E = 7565.60$ cm^{-1}; $\lambda = 1322$ nm.
[c] State $a = 4f^9 5d6s^2, {}^7\mathrm{I}^o_9$, $E = 9990.95$ cm^{-1}; $\lambda = 1001$ nm.
[d] State $a = 4f^9 5d6s^2, {}^5\mathrm{K}^o_9$, $E = 13495.92$ cm^{-1}; $\lambda = 741$ nm.

for dysprosium or to find magic wavelengths for other complex atoms. We demonstrate that many-body calculations and simple estimations give close results.

In the case of a narrow resonance, energy denominator in Eq. (1) is close to zero. This makes it possible to write an approximate formula for the magic frequency corresponding to this wavelength. Starting from the condition

$$\alpha_{\mathrm{GS}}(\omega^*) = \alpha_a(\omega^*) \tag{5}$$

and presenting dynamic polarizability of the excited state in the vicinity of the resonance n in the form

$$\alpha_a(\omega) = \alpha_a(0) - \frac{1}{3(2J_a+1)} \times \left[\frac{1}{E_a - E_n + \omega} + \frac{1}{E_a - E_n - \omega}\right] \langle a||\mathbf{D}||n\rangle^2, \tag{6}$$

we arrive at the following expression:

$$\omega^*_{an} = |E_a - E_n| + \frac{E_a - E_n}{|E_a - E_n|}\delta_n, \qquad \delta_n = \frac{1}{3(2J_a+1)} \frac{\langle a||\mathbf{D}||n\rangle^2}{[\alpha_{\mathrm{GS}}(\omega_n) - \alpha_a(0)]}, \tag{7}$$

where $\omega_n = |E_a - E_n|$ is the resonance frequency, n is the resonance number, $\langle a||\mathbf{D}||n\rangle$ is the electric dipole transition amplitude from the excited state a to the resonance state n, and $\alpha_{\mathrm{GS}}(\omega_n)$ is the scalar polarizability of the ground state at ω_n. Note that ω_n is the resonance frequency for the upper state, and the polarizability of the ground state usually changes very little in the vicinity of ω_n.

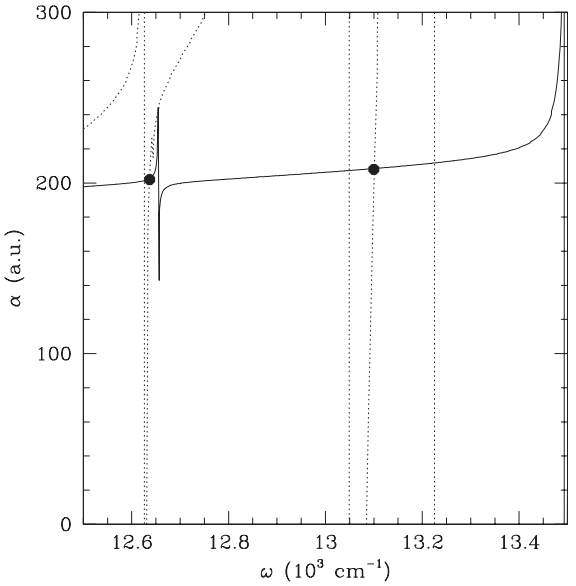

FIG. 1. Dynamic polarizability α of the ground state of Dy (solid line) and O1 (dotted line) between laser frequencies (wavelengths) 12 500 cm^{-1} (800 nm) and 13 500 cm^{-1} (741 nm). Lines cross at magic frequencies, and large dots correspond to the most useful frequencies.

In case of two closely spaced resonances in the upper-state polarizability, magic frequencies in the vicinity of resonance energies E_1 and E_2 can be found using the approximate

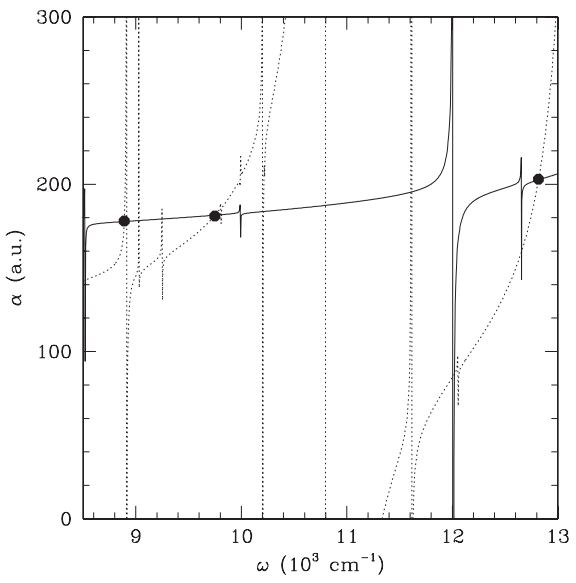

FIG. 2. Dynamic polarizability α of the ground state of Dy (solid line) and O2 (dotted line) between laser frequencies (wavelengths) 8500 cm^{-1} (1.18 μm) and 13 000 cm^{-1} (769 nm). Lines cross at magic frequencies, and large dots correspond to the most useful frequencies.

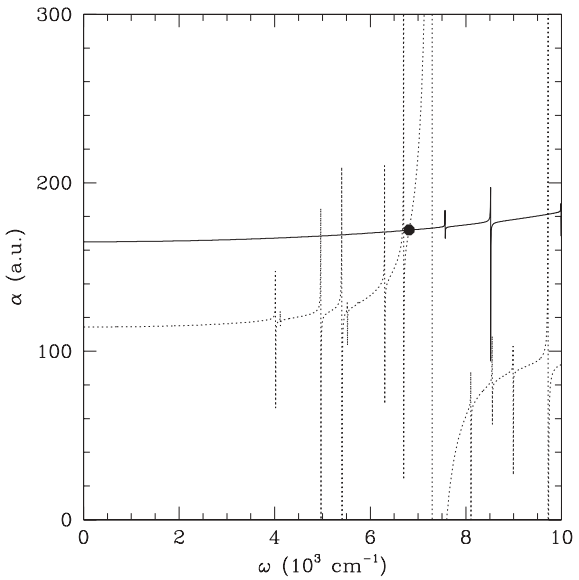

FIG. 3. Dynamic polarizability α of the ground state of Dy (solid line) and O3 (dotted line). Lines cross at magic frequencies, and the large dot corresponds to the most useful frequency.

formula

$$\omega^*_{a12} = \frac{E_1 + E_2}{2} + \delta_{12}, \tag{8}$$

where

$$\delta_{12} = \Delta_{12}\frac{C_J\Delta_{12}\left[\alpha^{(0)}_{\rm GS}(\omega_{12}) - \alpha^{(0)}_a(0)\right] + A_2^2 - A_1^2}{A_2^2 + A_1^2}. \tag{9}$$

Here $\Delta_{12} = (E_1 - E_2)/2$, $C_J = 3(2J_a + 1)$, $\omega_{12} = (E_1 + E_2)/2$, $A_1 = \langle a||\mathbf{D}||1\rangle$, and $A_2 = \langle a||\mathbf{D}||2\rangle$.

One does not need to know dynamic polarizability of an excited state to find magic frequencies using Eq. (7) or Eq. (8). However, one still needs to know the dynamic polarizability of the ground state and the relevant transition amplitudes. An approximate solution can be found using the following rules.

(i) The dynamic polarizability of the ground state is fitted very well within the energy interval from 0 to 0.05 a.u. by

$$\alpha_{\rm GS}(\omega) = \left(\frac{2.955}{\omega + 0.108\,15} - \frac{2.955}{\omega - 0.108\,15}\right) + 110 + 3000\omega^2. \tag{10}$$

We keep here numerical parameters for the dominant contribution to $\alpha_{\rm GS}$, which is due to the transition to the 421-nm state with energy $E = 23\,737\ {\rm cm}^{-1} = 0.108\,15$ a.u. This transition dominates due to the largest value of the transition amplitude: $\langle a||\mathbf{D}||n\rangle = 12.277$ a.u. (see Table I). The last two terms in Eq. (10) fit the contribution of all other transitions in the energy interval $0 < \omega < 0.05$ a.u. Resonances within this interval are ignored since they are too narrow for any practical importance.

(ii) Transition amplitudes can be estimated using approximate selection rules. If the difference of the total angular momentum L between two states is larger than 1 or if total spin S of the states is not equal, then the amplitude is not zero due to relativistic corrections but is likely to be small. One can use for a rough estimate $A = 0.1$ a.u. A similar estimation can be used if the transition is suppressed by configuration mixing, i.e., the transition between leading configurations cannot be reduced to a single-electron allowed electric dipole transition. If no selection rules are broken, the amplitude is likely to be large, and one can use $A = 3$ a.u. as a rough estimate.

(iii) Polarizability of the excited state at zero frequency can be estimated using Eq. (1) with experimental energies and with the amplitude estimated using the procedure in the previous paragraph.

This procedure can help in estimating magic wavelengths not only for the transitions considered in the present paper

TABLE III. Magic wavelengths λ^*, frequencies ω^* (cm^{-1}), and polarizabilities α for the three transitions in Dy.

Transition	Resonance $E_n - E_a$	δ_n[a]	δ_n[b]	Magic frequencies Formula	Calculations	λ^* (nm)	α (a.u.)
GS-O1	11 337	4		11 333	11 326	883	192
$E_a = 7566\ {\rm cm}^{-1}$	11 372	3		11 368	11 366	880	192
$\lambda = 1322$ nm	13 224	537		12 686	12 638	791	202
	13 136[c]		−35	13 101	13 100	763	208
GS-O2	7523	1		7522	7521	1330	172
$E_a = 9991\ {\rm cm}^{-1}$	7622	4		7617	7613	1314	174
$\lambda = 1001$ nm	8912	7		8905	8891	1125	178
					9749	1026	181
	13 227	483		12 744	12 817	780	203
GS-O3	5407	4		5403	5401	1850	163
$E_a = 13\,496\ {\rm cm}^{-1}$	6302	2		6300	6297	1588	171
$\lambda = 741$ nm	6697	4		6693	6671	1494	172
	7293	479		6814	6812	1468	172
	9722	8		9714	9716	1029	181

[a]Using formula (7), $\omega^*_{an} = E_n - E_a - \delta_n$.
[b]Using formulas (8) and (9), $\omega^*_{a12} = (E_1 + E_2)/2 - E_a + \delta_{12}$.
[c]$E_n = (20\,614 + 20\,790)/2 - 7566$.

but also for some other transitions. The main condition for it to work is that the magic wavelength should be close to a resonance so that the resonance term dominates in Eq. (1).

III. RESULTS

Table III shows the magic wavelengths and corresponding polarizabilities for the three transitions in Dy. We substitute calculated transition amplitudes from Table II when using the analytical formulas (7) and (8). The column marked as *calculations* presents magic frequencies that come from numerical calculations. Magic wavelengths in the next column correspond to calculated frequencies. Most of the magic frequencies are due to very narrow resonances and might be inconvenient for practical use due to optical dipole trap frequency instabilities and enhanced spontaneous emission. However, there are magic wavelengths for each of the three transitions where the resonance is not very narrow or even absent. They are $\lambda = 791$ nm ($\omega^* = 12\,638$ cm^{-1}) and $\lambda = 763$ nm ($\omega^* = 13\,100$ cm^{-1}) for the 1322-nm GS-O1 transition; $\lambda = 1125$ nm ($\omega^* = 8891$ cm^{-1}), $\lambda = 1026$ nm ($\omega^* = 9749$ cm^{-1}), and $\lambda = 780$ nm ($\omega^* = 12\,817$ cm^{-1}) for the 1001-nm GS-O2 transition; and $\lambda = 1029$ nm ($\omega^* = 9716$ cm^{-1}) and $\lambda = 1468$ nm ($\omega^* = 6812$ cm^{-1}) for the 741-nm GS-O3 transition.

The magic frequency $\omega^* = 13\,100$ cm^{-1} for the GS-O1 transition is between two close resonances at $\omega = 13\,149$ cm^{-1} and $\omega^* = 13\,224$ cm^{-1} that correspond to transitions from the $^7H_8^o$ state at $E = 7566$ cm^{-1} to the close states of the $4f^9 6s^2 6p_{1/2}$ configuration at $E = 20\,614$ cm^{-1} and $E = 20\,789$ cm^{-1}. Using formulas (8) and (9) gives a very accurate estimate of the magic frequency (see Table III). It is interesting to note that there is a frequency interval for the GS-O1 transition where polarizabilities of two states come very close to each other but do not cross: $\delta\alpha/\alpha \leqslant 2\%$ for $12\,121 < \omega < 12\,183$ cm^{-1}.

The magic wavelengths $\lambda = 780$ and 1026 nm for the GS-O2 transition and $\lambda = 1468$ nm for the GS-O3 transition do not correspond to any very close resonance, and the values of the polarizabilities coincide by chance rather than due to a resonance. Therefore, these magic wavelengths are the least sensitive to laser frequency fluctuations and are the most promising for resolved-sideband cooling, precision measurement, and QIP applications. The GS-O2 transition magic wavelengths can be reached with high optical power using a Ti:sapphire or tapered amplified diode laser for 780 nm and a diode laser or fiber laser for 1026 nm. The GS-O3 transition magic wavelength at 1468 nm could be reached with a low-power diode laser, which could perhaps be doped-fiber amplified, and the 1029-nm wavelength could be reached with a fiber laser.

Future work will explore the role of laser polarization on the magic wavelength position. Such a calculation is beyond the scope of this present work, but we estimate that the shifts will be small since the magic wavelengths for unpolarized light occur in proximity to resonances.

Optical dipole traps at these wavelengths, far from the broad Dy transitions, would be suitable for lattice confinement in the Lamb-Dicke regime without undue heating. For example, one-dimensional lattice confinement at the 780-nm magic wavelength with 0.5 W provides ample trap depth with sub-1-Hz scattering rates. With larger laser intensities, suitable trap depths and low scattering rates can be achieved at the other magic wavelengths. Vibrational spacing can be many tens of kilohertz, which is large enough for resolved-sideband cooling on the 2-kHz-wide 741-nm transition [28]. For rapid cooling, the 50-Hz-wide 1001-nm transition, much narrower than any trap frequencies in a typical three-dimensional (3D) optical lattice, would need to be broadened via a quenching transition [22], and the optical dipole trap magic wavelength would need to be adjusted to compensate the Stark shift from the quenching laser. Resolved-sideband cooling on these narrow transitions in a 3D optical lattice may provide an alternative route to quantum degeneracy [29] versus evaporative cooling, which may fail due to (as yet unmeasured) unfavorable scattering properties in this highly dipolar gas.

ACKNOWLEDGMENTS

We thank J. Ye, I. Deutsch, and N. Burdick for discussions. The work was funded in part by the Australian Research Council (V.A.D., V.V.F.), the NSF (Grant No. PHY08-47469) (B.L.L.), AFOSR (Grant No. FA9550-09-1-0079) (B.L.L.), and the Army Research Office MURI award W911NF0910406 (B.L.L.).

[1] V. A. Dzuba, V. V. Flambaum, and I. B. Khriplovich, Z. Phys. D At. Mol. Clusters **1**, 243 (1986).
[2] V. A. Dzuba, V. V. Flambaum, and M. G. Kozlov, Phys. Rev. A **50**, 3812 (1994).
[3] D. Budker, D. DeMille, E. D. Commins, and M. S. Zolotorev, Phys. Rev. A **50**, 132 (1994).
[4] A. T. Nguyen, D. Budker, D. DeMille, and M. Zolotorev, Phys. Rev. A **56**, 3453 (1997).
[5] V. A. Dzuba and V. V. Flambaum, Phys. Rev. A **81**, 052515 (2010).
[6] V. A. Dzuba, V. V. Flambaum, and J. K. Webb, Phys. Rev. Lett. **82**, 888 (1999).
[7] V. A. Dzuba, V. V. Flambaum, and J. K. Webb, Phys. Rev. A **59**, 230 (1999).
[8] V. A. Dzuba, V. V. Flambaum, and M. V. Marchenko, Phys. Rev. A **68**, 022506 (2003).
[9] A.-T. Nguyen, D. Budker, S. K. Lamoreaux, and J. R. Torgerson, Phys. Rev. A **69**, 022105 (2004).
[10] A. A. Cingöz, A. Lapierre, A.-T. Nguyen, N. Leefer, D. Budker, S. K. Lamoreaux, and J. R. Torgerson, Phys. Rev. Lett. **98**, 040801 (2007).
[11] V. A. Dzuba and V. V. Flambaum, Phys. Rev. A **77**, 012515 (2008).
[12] S. J. Ferrell, A. Cingöz, A. Lapierre, A.-T. Nguyen, N. Leefer, D. Budker, V. V. Flambaum, S. K. Lamoreaux, and J. R. Torgerson, Phys. Rev. A **76**, 062104 (2007).
[13] M. Lu, S. H. Youn, and B. L. Lev, Phys. Rev. Lett. **104**, 063001 (2010).

[14] N. Leefer, A. Cingöz, D. Budker, S. J. Ferrell, V. V. Yashchuk, A. Lapierre, A.-T. Nguyen, S. K. Lamoreaux, and J. R. Torgerson, in *Proceedings of the 7th Symposium Frequency Standards and Metrology, Asilomar, October 2008*, edited by L. Maleki (World Scientific Singapore, 2009), pp. 34–43.
[15] N. Leefer, A. Cingöz, B. Gerber-Siff, A. Sharma, J. R. Torgerson, and D. Budker, Phys. Rev. A **81**, 043427 (2010).
[16] S.-H. Youn, M. Lu, U. Ray, and B. L. Lev, Phys. Rev. A **82**, 043425 (2010).
[17] S.-H. Youn, M. Lu, and B. L. Lev, Phys. Rev. A **82**, 043403 (2010).
[18] A. J. Berglund, J. L. Hanssen, and J. J. McClelland, Phys. Rev. Lett. **100**, 113002 (2008).
[19] F. Diedrich, J. C. Bergquist, W. M. Itano, and D. J. Wineland, Phys. Rev. Lett. **62**, 403 (1989).
[20] T. Ido and H. Katori, Phys. Rev. Lett. **91**, 053001 (2003).
[21] J. Ye, H. J. Kimble, and H. Katori, Science **320**, 1734 (2008).
[22] Ch. Grain, T. Nazarova, C. Degenhardt, F. Vogt, Ch. Lisdat, E. Tiemann, U. Sterr, and F. Riehle, Eur. Phys. J. D **42**, 317 (2007).
[23] V. A. Dzuba and V. V. Flambaum, Phys. Rev. A **77**, 012514 (2008).
[24] T. M. Miller, in *Handbook of Chemistry and Physics*, edited by D. R. Lide (CRC, Boca Raton, 2000), p. E-71.
[25] V. A. Dzuba, V. V. Flambaum, P. G. Silvestrov, and O. P. Sushkov, J. Phys. B **20**, 1399 (1987).
[26] V. A. Dzuba, V. V. Flambaum, J. S. M. Ginges, and M. G. Kozlov, Phys. Rev. A **66**, 012111 (2002).
[27] W. R. Johnson and J. Sapirstein, Phys. Rev. Lett. **57**, 1126 (1986).
[28] M. Lu, S.-H. Youn, and B. L. Lev, Phys. Rev. A **83**, 012510 (2011).
[29] M. Olshanii and D. Weiss, Phys. Rev. Lett. **89**, 090404 (2002).